

## THE IMPROVEMENT OF MONTMORILLONITE ACTIVITY IN 2-BUTANOL DEHYDRATION BY METAL OXIDE PILLARIZATION

I. FATIMAH\*, M. RAPEI

Chemistry Department, Universitas Islam Indonesia, Kampus Terpadu UII, Jl. Kaliurang  
Km 14, Sleman, Yogyakarta Indonesia 55584

\*Corresponding Author: isfatimah@uii.ac.id

### Abstract

Heterogeneous catalysis based on the utilization of natural inorganic material is widely investigated. Among other materials, clay exhibiting interesting physicochemical properties due to its surface area and acidity, but the use of clay facing to the fact that it is not thermal stable in high temperature. In this paper, the improvement on clay properties by pillarization process and study of its role in 2-butanol dehydration were presented. Research steps consist of aluminium oxide, titanium oxide and zinc oxide pillarization to activated natural montmorillonite followed by activity test of pillared material in 2-butanol dehydration. A fluidized bed reactor was used for the catalytic testing and GCMS analysis of the products was performed for the evaluation of catalytic activity, total conversion and the selectivity of the product. Several physicochemical characterization techniques of material were studied by DTA-TGA, XRD, BET surface area analysis and surface acidity. The role of surface acidity and also pore distribution of the catalysts towards the improvement of 2-butanol conversion into 2-butene and di-sec butyl ether is discussed in this paper.

Keywords: Alcohol dehydration, Clay, Pillarization, Nickel catalyst.

### 1. Introduction

Alcohol dehydration is an important reaction in chemical industry, for example in the synthesis of ether as chemical intermediate for other valuable chemical synthesis. Dehydration of methanol in dimethyl ether (DME) for example is considered the fuel for 21st Century as it can be applied as substituent for alternative energy [1]. The reaction requires a high active and selective catalyst. For clean, economic and green chemical purposes the preparation of heterogeneous catalysts for alcohol dehydration are afforded. Some research groups tried to prepare bifunctional catalyst by getting together both dehydration

**Nomenclatures**

<i>B/L</i>	Ratio of Broensted to Lewis acidity
<i>I</i>	Intensity
<i>P/P<sub>0</sub></i>	Ratio of measured pressure to initial pressure in gas sorption analysis

**Abbreviations**

Al-MMT	Aluminium-pillared montmorillonite
BET	Brunair-Emmet-Teller
CEC	Cation exchange capacity
DME	Dimethyl ether
JCPDS	Joint Committee on Powder Diffraction Standards
MMT	Montmorillonite
Ti-MMT	Titanium-pillared montmorillonite
Zn-MMT	Zinc-pillared montmorillonite

and hydrogenation sites in the same catalyst. Acidity and thermal stability are the physical properties that can support the reaction mechanism [2]. By these properties such silica alumina based catalysts are reported from some previous investigations. Considering the high potency of clay minerals in Indonesia, this research aimed to prepare catalyst based on clay for alcohol dehydration; especially 2-butanol dehydration in order to evaluate the comparison on physicochemical properties of metal oxide pillared clay and its relationship with the catalytic activity especially as acid catalyst.

When inorganic species are introduced into the interlayers of the clay, the resulting nanocomposite can be used as a catalyst with high surface area and high thermal stability. Pillared interlayered clay catalyst can be prepared by the insertion of metal clusters precursor such as (Zr, Zn and Ti) that will generate larger than those of zeolites. Study on the activity of pillared clays with varied preparation variables have thus been evaluated in the literature. Based on some review on the surface acidity, pillaring metal of Zr, Zn and Ti were reported to be excellent in increasing the solid activity in acid controlled reaction. This research deals with study on physicochemical character of Al, Ti and Zn pillared montmorillonite clay and its evaluation as acid catalyst in 2-butanol dehydration reaction.

**2. Materials and Method****2.1. Materials:**

Montmorillonite clay (furthermore encoded as MMT) with a cation exchange capacity (CEC) of 99.0 mequiv./100 g of clay was purchased from PT.Tunas Inti makmur Company, Semarang, Indonesia. Analytical grade aluminium chloride hexahydrate, zinc acetate, titanium oxide chloride, NaOH, 2-butanol were obtained from Merck-Millipore.

**2.2. Material preparation**

Metal oxide pillared clay catalysts were prepared using natural montmorillonite as raw material. The aluminium oxide, titanium oxide and zinc oxide pillarization

toward montmorillonite were conducted with the metal to clay ratio of 10 mmol/gram by specified procedure for each pillarization as follow:

- a) For aluminium pillarization, pillaring agent of  $Al_{13}$  Keggin ions was synthesized by slow titration of 0.5 M into a solution of 0.5 M  $AlCl_3 \cdot 6H_2O$  at room temperature with a -OH/Al mole ratio of 2.2 followed by stirring for 24 hours. The pillaring agent was then dispersed into montmorillonite suspension and the mixture was then refluxed for 6h before filtration, neutralization and calcination. Obtained material by these treatments was called as aluminium pillared montmorillonite and was encoded as Al-PILM.
- b) For zinc oxide pillarization, the procedure was the same as was reported before [3].
- c) For titanium oxide pillarization was employed by using  $TiOCl_2$  as precursor. The pillaring solution was obtained by diluting  $TiOCl_2$  with HCl followed by stirring for 4 h before the dispersion into montmorillonite suspension. The mixture was then refluxed for 8h before filtration, neutralization and calcination.

The materials obtained were encoded as Al-PILM, Zn-PILM and Ti-PILM respectively.

### 2.3. Characterization

Physicochemical character of pillared materials were obtained through X-ray diffraction (XRD) analysis, SEM-EDX, BET surface area analyzer and diffuse reflectance spectrophotometry (DRUV-Vis). XRD Shimadzu X6000 with Ni-filtered  $Cu-K_{\alpha}$  radiation source, the range of 2-60 $\theta$  and the stepsize of 4  $^{\circ}$ /min was used. Based on the analysis data of XRD, the information on crystallinity of the material, the change of basal spacing  $d_{001}$  produced by pillarization as well as the presence / absence of metal oxide crystalline phase formation were studied. Analysis using the BET surface area analyzer NOVA 1200 surface area will provide data specific surface area, pore size distribution and average pore radius.

Diffuse reflectance spectra of finely ground pillared montmorillonite samples were obtained in the ultraviolet-visible (UV-vis) range using a JASCO spectrometer with Scientific diffuse reflectance attachment and a controlled environment reaction chamber. Reflectance/absorbance measurements were converted into absorbance units using the Kubelka-Munk function.

The reaction of 2-butanol dehydration was carried out at atmospheric pressure over pure solid-acid catalysts. The reactions were conducted under differential temperature and the liquid products obtained from each running were collected for GCMS analysis.

### 3. Results and Discussion

The XRD patterns of raw material and pillared materials are shown in Fig. 1. There were strong peaks at  $2\theta = 6,30^{\circ}$  ( $d_{001} = 14,47 \text{ \AA}$ ) and  $2\theta = 19,89^{\circ}$  ( $d_{002} = 4,46 \text{ \AA}$ ). Generally montmorillonite clay shows the  $d_{001}$  basal spacing at around 30  $\text{\AA}$  and 3  $\text{\AA}$  that are coincide with the angle at around  $2^{\circ}$  and  $30^{\circ}$ . Refer to *Joint Committee on Powder Diffraction Standards* (JCPDS) data, the intensity at  $2\theta=6,10^{\circ}$  gives the relative intensity of 100% and the reflection at  $d_{002}$

(4,46Å) has relative intensity of 60-80%. Other reflections at  $2\theta = 20,68^\circ$  and  $26,5^\circ$  with the intensity ratio  $I_{26,5} / I_{20,68} = 1/0.2$  indicate the presence of quartz as impurities in natural minerals. The incorporation metal oxide caused the different displacements in the basal spacing and the value of  $d_{001}$  are tabulated in Table 1. The typical basal spacing which is the characteristic of smectite groups was increased to around 15.38 Å-16.53Å after pillarization. These observations established the fact of successful pillarization of metal oxide into the interlayer space of montmorillonite and the incorporation of metal oxide into clay mineral. The formation of crystalline metal oxide was shown by the reflections of anatase and zinc oxide phase for Ti-PILM and Zn-PILM while for Al-PILM there are no additional reflection appeared. ZnO in wurtzite phase is proven by the reflections at  $31.6; 32.6$  and  $36.3^\circ$  that are assigned to (100); (002) and (101) plane [3]. From Ti-PILM the formation of  $TiO_2$  phase is indicated from the reflection at around  $25^\circ; 52^\circ$  and  $64^\circ$  that correspond to anatase form and around  $22^\circ$  from rutile phase [4].

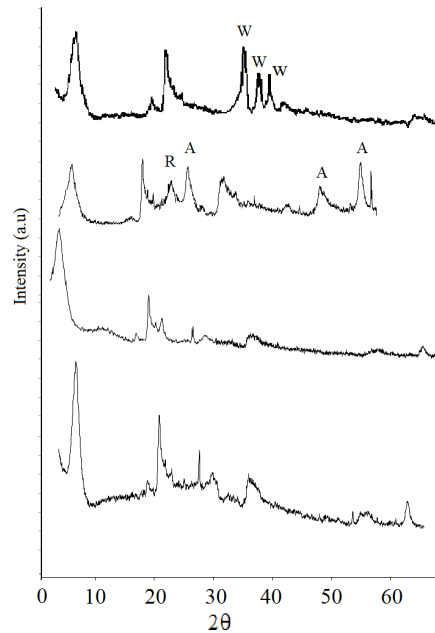


**Fig.1. XRD pattern of MMT, Al-PILM, Ti-PILM and Zn-PILM.**  
(W: Wurtzite, A: anatase; R: Rutile)

**Table 1. Calculated  $d_{001}$  of montmorillonite and pillared montmorillonite.**

Sampel	$d_{001}$ (nm)	Relative Intensity (%)
MMT	14.89	100.00*
Al-PILM	16.53	110
Ti -PILM	15.38	38.12
Zn-PILM	15.09	89.99

\*Compared to  $I_{d_{001}}$  of MMT

The nitrogen adsorption-desorption isotherms of materials are shown in Fig. 2. All samples shows that the isotherms are correspond to the Type II isotherm for mesoporous materials according to the International Union of Pure and Applied Chemistry (IUPAC) classification. Nitrogen fill a monolayer at relatively low pressures followed by buildup multilayers until capillary condensation sets in illustrates a typical monolayer and multilayer adsorption on solids with a heterogeneous surface, predominantly macro and mesoporous structures. The pattern of adsorption-desorption profile of Al-PILM and Zn-PILM seems similar in that the the hysteresis loops suggests the formation of mesoporous structure as result of pillarization that probably comes from the formation of interlayer space between metal oxide pillar, while the pattern from Ti-PILM is slightly different with both [5]. The hysteresis of Ti-PILM is type H3 (IUPAC classification), which confirms that the slit shape layered structure was maintained, but was disordered in form and size [6].

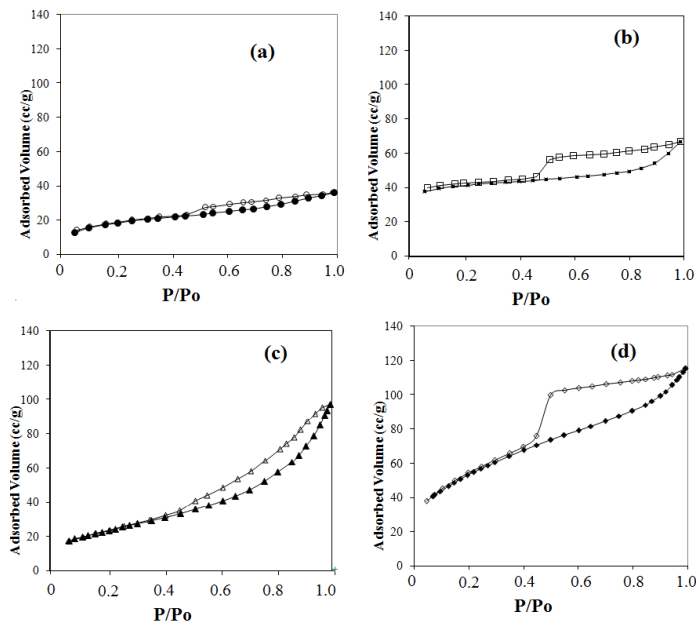


**Fig. 2. Adsorption-desorption profile of (a) MMT, (b) Al-PILM, (c) Ti-PILM, (d) Zn-PILM.**

Based on adsorption data, the parameter of specific surface area, pore volume and pore radius are listed in Table 2. The specific surface area increases from 45.96 to 110.34  $\text{m}^2 \text{g}^{-1}$  in the Ti-PILM which is the highest value of specific surface area amongst pillared materials.

**Table 2. Surface profile of MMT and pillared materials.**

Sample	Specific Surface Area ( $\text{m}^2 \text{g}^{-1}$ )	Pore Volume ( $\times 10^{-3} \text{cc/g}$ )	Pore Radius ( $\text{\AA}$ )
MMT	45.90	0.521	14.98
Al-PILM	79.09	21.080	15.30
Ti-PILM	110.34	19.80	11.78
Zn-PILM	98.20	10.98	10.30

These data show a significant increase of the BET surface area and pore volume of pillared material samples compared with the starting material. The evident increase in surface area and total pore volume is to be related to the formation of metal oxide pillars between octahedral sheet structures of MMT. The different values at different precursor indicate the different interaction between pillaring complex and the surface of montmorillonite.

Effect of the insertion of metal oxide into clay structure is also studied by DRUV-Vis spectrophotometric analysis. The spectra is depicted in Fig.3 and calculated band gap energy ( $E_g$ ) of the samples are tabulated in Table 3. From the spectra it can be seen that pillared materials have higher absorption along UV range which reflects charge transfer ability of  $TiO_2$  and  $ZnO$  as semiconductor and also indicate the presence of larger number of aluminum (III) in the in the formation of the crystal lattice of the pillared clay.

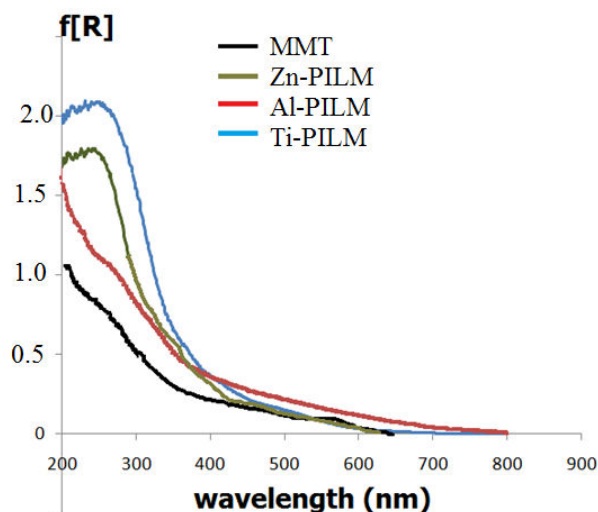


Fig. 3. DRUV-Vis spectra of pillared materials and MMT.

### 3.1. Surface acidity

Surface acidity of MMT and pillared materials is evaluated by using pyridine adsorption followed by FTIR measurement. The spectra of pyridine-adsorbed materials is presented in Fig.4. Pyridine molecule was utilized as probe molecule for this evaluation. The detection of adsorbed pyridine represents the amount of acid sites of material surface. The typical interactions observed when pyridine is adsorbed and there are two specific interaction, i.e, Lewis interaction where nitrogen of pyridine was bonded to proton from surface and Broensted interaction between aromatic ring of pyridine with the proton from the surface. Lewis interaction can be recorded by the corresponding band at around  $1450\text{ cm}^{-1}$  while the Broensted interaction is at around  $1540\text{ cm}^{-1}$ , so the ratio of Broensted to Lewis acidity (B/L) can be measured from the value of intensity of both bands [7-9]. Table 3 shows the B/L ratio and total acidity of materials. Both B/L and total surface acidity increases as result of metal oxide insertion.

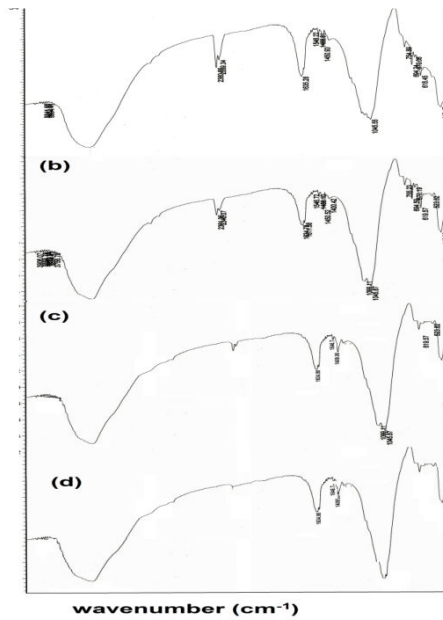


Fig. 4. FTIR spectra of pyridine adsorbed materials (a) Zn-PILM, (b) Ti-PILM, (c) Al-PILM, (d) MMT.

Table 3. B/L ratio and total acidity of materials.

Sample	Acidity (mmol pyridin/g)	Total Acidity (mg butylamine/g)	B ratio
MMT	0.460	0.775	0.99
Al-PILM	0.760	1.110	1.09
Ti-PILM	0.813	1.433	1.23
Zn-PILM	0.780	1.413	1.09

The profile of the catalytic activity of materials in 2-butanol dehydration is represented by catalyst activity, total conversion and selectivity towards di-sec butyl ether in the product of reaction (Table 3) by following Eqs. (1) - (3):

$$\text{Total Conversion(\%)} = \frac{\text{mole of } [2\text{-butanol}]_i - [2\text{-butanol}]_p}{\text{mole of } [2\text{-butanol}]_i} \times 100\% \quad (1)$$

$$\text{Catalyst Activity(\%)} = \frac{\text{mole of } 2\text{-butanol reacted to form product}}{\text{mole of } 2\text{-butanol reacted}} \times 100\% \quad (2)$$

$$\text{Selectivity of product } i(\%) = \frac{\text{mole of } [\text{Product}-i]}{\text{mole of reacted } 2\text{-butanol}} \times 100\% \quad (3)$$

where  $[2\text{-butanol}]_o$ ,  $[2\text{-butanol}]_p$  are peak area of 2-butanol in feed and product respectively.

Data in Table 4 shows that all parameters of 2-butanol dehydration reaction over pillared materials are higher compared to raw montmorillonite. It is clear that the insertion of metal oxide in catalyst causes the higher content of surface acidity that plays role in surface mechanism. All physicochemical character of pillared materials are in linear correlation with the reaction parameter. According to the results of the catalytic evaluation by means 2-butanol dehydration a correlation could establish among the ratio Lewis/Bronsted and the surface parameter to catalyst activity and selectivity toward di-sec butyl ether. The higher the specific surface area of material, the higher the B/L ratio and total acidity and these are synergistically enhance the conversion and the catalyst activity. By these correlation the catalytic activity of pillared materials are in following order Ti-PILM>Zn-PILM>Al-PILM > MMT. The strong relationship between surface parameter including surface area and surface acidity was reported by previous investigation [10]. From the selectivity data, it is also noted that Ti-PILM gives highest selectivity towards 2-butene formation as a main product targeted from the reaction mechanism [11, 12]. The selectivity is controlled by surface adsorbability to the intermediate i.e carbocation of 2-butanol that is formed. Effective interaction between carbocations produce 2-butene.

**Table 4. Catalyst activity, total conversion and selectivity towards 2-butene of 2-butanol dehydration over MMT and pillared materials.**

Sample	Conversion (%)	Catalyst Activity	Selectivity 2-butene
MMT	45.00	19.8	25.4
Al-PILM	78.47	62.5	45.7
Ti-PILM	98.45	87.9	98.00
Zn-PILM	90.38	78.5	94.3

\*Reaction condition: Temperature : 300 °C

Furthermore, thermodynamic study was conducted by evaluating effect of temperature on catalytic performance of Ti-PILM. The trend is presented by Fig. 5. The conversion and catalyst activity are enhanced at elevated temperature suggest that temperature gives influence to the adsorption of 2-butanol as well as the rate of intermediate formation as rate determining step within the mechanism. However the difference between the results from temperature of 600 and 700°C are not significant. However the temperature gives no effect to the catalyst selectivity toward di sec-butyl ether formation.

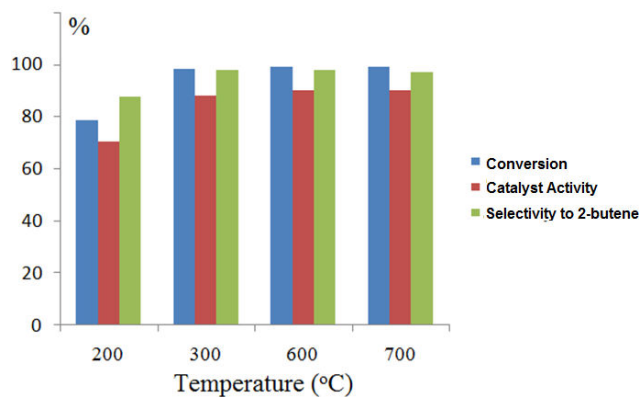


**Fig. 5. Catalyst profile of Ti-PILM at varied temperature.**



#### 4. Conclusion

Preparation of Al, Ti and Zn oxide pillared montmorillonite has been conducted. Prepared materials were found to have better physicochemical character that support the mechanism of 2-butanol dehydration reaction. The activity of pillared materials as catalysts in 2-butanol dehydration reaction was found to be determined mainly by the surface profile and surface acidity. As a comparison among pillared materials, the activity is in following order: Ti-PILM>Zn-PILM>Al-PILM > MMT.

#### References

1. Baertsch, C. (2002). Genesis of brønsted acid sites during dehydration of 2-butanol on tungsten oxide catalysts. *Journal of Catalysis*, 205(1), 44-57.
2. West, R.M.; Braden, D.J.; and Dumesic, J.A. (2009). Dehydration of butanol to butene over solid acid catalysts in high water environments. *Journal of Catalysis*, 262(1), 134-143.
3. Fatimah, I.; and Huda, T. (2012). Indonesian montmorillonite-supported ZnO: preparation, characterization and activity test in methanol dehydration. *Asian Journal of Material Sciences*, 4, 13-20.
4. Paul, B.; Martens, W.N.; and Frost, R.L. (2012). Immobilised anatase on clay mineral particles as a photocatalyst for herbicides degradation. *Applied Clay Science*, 57, 49-54.
5. Ayodele, O.B.; Lim, J.K.; and Hameed, B.H. (2012). Pillared montmorillonite supported ferric oxalate as heterogeneous photo-Fenton catalyst for degradation of amoxicillin. *Applied Catalysis A: General.*, 413, 301-309.
6. Kitayama, Y.; Kodama, T.; Abe, M.; and Shimotsuma, H. (1998). Synthesis of titania pillared saponite in aqueous solution of acetic acid. *Journal of Porous Materials*, 5(2), 121-126.
7. Frenkel, M. (1974). Surface acidity of montmorillonites. *Clays and Clay Minerals*, 22(5-6), 415-441.
8. Akçay, M. (2005). The surface acidity and characterization of Fe-montmorillonite probed by in situ FT-IR spectroscopy of adsorbed pyridine. *Applied Catalysis A: General*, 294(2), 156-160.
9. Tyagi, B; Chudasama, C.D.; and Jasra, R.V. (2006). Characterization of surface acidity of an acid montmorillonite activated with hydrothermal, ultrasonic and microwave techniques. *Applied Clay Science*, 31(1), 16-28.
10. Ramos, F.S.; de Farias, A.D.; Borges, L.E.P.; Monteiro, J.L.; Fraga, M.A.; Sousa-Aguiar, E.F.; and Appel, L.G. (2005). Role of dehydration catalyst acid properties on one-step DME synthesis over physical mixtures. *Catalysis Today*, 101(1), 39-44.
11. Jeong, S.; Kim, H.; Bae, J.; Kim, D.H.; Peden, C.H.F.; Park, Y.K.; and Jeon, J.K. (2012). Synthesis of butenes through 2-butanol dehydration over mesoporous materials produced from ferrierite. *Catalysis Today*, 185(1), 191-197.
12. Baertsch, C.D.; Komala, K.T.; Chua, Y.H.; and Iglesia, E. (2002). Genesis of brønsted acid sites during dehydration of 2-butanol on tungsten oxide catalysts. *Journal of Catalysis*, 205(1), 44-57.